Monthly Notices of the ROYAL ASTRONOMICAL SOCIETY

MNRAS **513,** L40–L45 (2022) https://doi.org/10.1093/mnrasl/slac030
Advance Access publication 2022 March 25

The synchronized dance of the magellanic clouds' star formation history

P. Massana [1,2★] T. Ruiz-Lara [3★] N. E. D. Noël,[1] C. Gallart,[4,5] D. L. Nidever,[6] Y. Choi [7] J. D. Sakowska [1] G. Besla,[8] K. A. G. Olsen,[9] M. Monelli [4,5] A. Dorta,[4] G. S. Stringfellow [10] S. Cassisi,[11,12] E. J. Bernard,[13] D. Zaritsky [8] M.-R. L. Cioni [14] A. Monachesi [15,16] R. P. van der Marel,[7,17] T. J. L. de Boer[18] and A. R. Walker[19]

[1]*Department of Physics, University of Surrey, Guildford GU2 7XH, UK*
[2]*Isaac Newton Group of Telescopes, Apartado 321, E-38700 Santa Cruz de La Palma, Canary Islands, Spain*
[3]*Kapteyn Astronomical Institute, University of Groningen, Landleven 12, NL-9747 AD Groningen, The Netherlands*
[4]*Instituto de Astrofísica de Canarias, Calle Vía Láctea s/n, E-38205 La Laguna, Tenerife, Spain*
[5]*Departamento de Astrofísica, Universidad de La Laguna, E-38200 La Laguna, Tenerife, Spain*
[6]*Department of Physics, Montana State University, P.O. Box 173840, Bozeman, MT 59717-3840, USA*
[7]*Space Telescope Science Institute, 3700 San Martin Drive, Baltimore, MD 21218, USA*
[8]*Steward Observatory, University of Arizona, 933 North Cherry Avenue, Tucson, AZ 85721, USA*
[9]*NSF's National Optical-Infrared Astronomy Research Laboratory, 950 N. Cherry Ave., Tucson, AZ 85719, USA*
[10]*Center for Astrophysics and Space Astronomy, University of Colorado, 389 UCB, Boulder, CO 80309-0389, USA*
[11]*INAF-Osservatorio Astronomico d'Abruzzo, via M. Maggini, sn., I-64100 Teramo, Italy*
[12]*INFN - Sezione di Pisa, Largo Pontecorvo 3, I-56127 Pisa, Italy*
[13]*OCA, CNRS, Université Côte d'Azur, Lagrange, Bd de l'Observatoire, CS 34229, F-06304 Nice cedex 4, France*
[14]*Leibniz-Institut für Astrophysik Potsdam (AIP), An der Sternwarte 16, D-14482 Potsdam, Germany*
[15]*Instituto de Investigación Multidisciplinario en Ciencia y Tecnología, Universidad de La Serena, Raúl Bitrán 1305, La Serena, 1720256, Chile*
[16]*Departamento de Astronomía, Universidad de La Serena, Av. Juan Cisternas 1200 N, La Serena, 1720236, Chile*
[17]*Center for Astrophysical Sciences, Department of Physics & Astronomy, Johns Hopkins University, Baltimore, MD 21218, USA*
[18]*Institute for Astronomy, University of Hawai'i, 2680 Woodlawn Drive, Honolulu, HI 96822, USA*
[19]*Cerro Tololo Inter-American Observatory, NSF's NOIRLab, Casilla 603, La Serena, 1700000, Chile*

Accepted 2022 March 14. Received 2022 March 10; in original form 2021 August 11

ABSTRACT

We use the SMASH survey to obtain unprecedented deep photometry reaching down to the oldest main-sequence turn-offs in the colour–magnitude diagrams (CMDs) of the Small Magellanic Cloud (SMC) and quantitatively derive its star formation history (SFH) using CMD fitting techniques. We identify five distinctive peaks of star formation in the last 3.5 Gyr, at ∼3, ∼2, ∼1.1, ∼0.45 Gyr ago, and one presently. We compare these to the SFH of the Large Magellanic Cloud (LMC), finding unequivocal synchronicity, with both galaxies displaying similar periods of enhanced star formation over the past ∼3.5 Gyr. The parallelism between their SFHs indicates that tidal interactions between the MCs have recurrently played an important role in their evolution for at least the last ∼3.5 Gyr, tidally truncating the SMC and shaping the LMC's spiral arm. We show, for the first time, an SMC–LMC correlated SFH at recent times in which enhancements of star formation are localized in the northern spiral arm of the LMC, and globally across the SMC. These novel findings should be used to constrain not only the orbital history of the MCs but also how star formation should be treated in simulations.

Key words: galaxies: interactions – evolution – Magellanic Clouds – galaxies: photometry – galaxies: star formation.

1 INTRODUCTION

Close galaxy encounters are expected to induce star formation (Ellison et al. 2013) and, as such, side-by-side examinations of star formation histories (SFHs) of two or more interacting systems can provide important insights into their orbital history. This, in turn, can help constrain the specifics of the star formation triggering mechanisms and the star formation recipes in galaxy evolution models.

Located at respective distances of ∼50 kpc (Pietrzyński et al. 2019) and ∼62.5 kpc (Graczyk et al. 2020) from the Sun, the Large and Small Magellanic Clouds (LMC/SMC) are the nearest interacting pair of dwarf galaxies. Their closeness makes them excellent laboratories to obtain SFHs in splendid detail, while they also offer the opportunity to derive accurate stellar radial velocities (Carrera et al. 2017; Cullinane et al. 2020; De Leo et al. 2020), proper motions (Kallivayalil et al. 2013; Schmidt et al. 2020; Gaia Collaboration et al. 2021) and gas distributions (Nidever et al. 2010). Since all these observables are key to constraining their orbits, the MCs are ideal systems to study the effects of tidal interactions on galaxy evolution. However, with the current observational accuracy,

★ E-mail: pol.massana@montana.edu (PM); t.ruiz.lara@rug.nl (TR-L)

© 2022 The Author(s)
Published by Oxford University Press on behalf of Royal Astronomical Society

Downloaded from https://academic.oup.com/mnrasl/article/513/1/L40/6554248 by Biblioteca P. Arduino user on 24 June 2022

the main drivers of uncertainty in the LMC/SMC and Magellanic Clouds (MCs) / Milky Way (MW) orbits are their still not well-constrained total masses (see e.g. Patel et al. 2020). Therefore, the SFHs of the LMC and the SMC are key sources of information not only of their internal evolution but also potentially powerful tools to further constrain their interaction history.

The LMC's SFH presents multiple episodes of star formation with several recent enhancements (Harris & Zaritsky 2009; Monteagudo et al. 2018; Ruiz-Lara et al. 2020b; Mazzi et al. 2021) that are possibly the products of interactions. Also, the age distribution of the LMC's cluster population seems to correlate with its global SFH, with two major periods of star and cluster formation, one at old ages (∼12–13.7 Gyr ago) and another in the past 3 Gyr (e.g. Olszewski et al. 1991; Ruiz-Lara et al. 2020b). However, while some activity at intermediate-ages is found in the field SFH, there is only one cluster of intermediate-age in the LMC (Mackey et al. 2016), which could have been accreted from the SMC (Bekki & Chiba 2007). The SMC SFH has been found to be characterized by several recent enhancements at ∼50 Myr ago, ∼100–250 Myr ago, ∼1–3 Gyr ago (Harris & Zaritsky 2004; Noël et al. 2007, 2009; Rubele et al. 2018), with ongoing star formation in the SMC 'wing' and eastern parts (Noël et al. 2009; Cignoni et al. 2012). However, it does not show conspicuous field star formation at early epochs (Rubele et al. 2018), something supported by the presence of only a single old globular cluster, NGC 121, that is considerably younger than the MW's globular clusters (∼11.2 Gyr; Glatt et al. 2008).

Traditionally thought to have had repeated pericentric passages around the MW (e.g. Brüns et al. 2005; Mastropietro et al. 2005), precise proper motions (Kallivayalil et al. 2006a; Kallivayalil, van der Marel & Alcock 2006b) have shown instead that the MCs are most likely on their first infall into our Galaxy's potential and that they must have been interacting with each other for some time (Patel et al. 2020). For instance, the Magellanic Bridge, a feature comprised of stars and gas connecting both the LMC and the SMC (Hindman, Kerr & McGee 1963; Noël et al. 2013, 2015), likely formed during a recent (∼150–200 Myr ago) close approach (Zivick et al. 2018) between the Clouds. However, owing to proper motion, distance, and modelling uncertainties, it remains unknown where in the LMC disc that recent close encounter occurred or how many encounters there have been in the past.

To shed light on whether interactions between the LMC and the SMC have triggered star formation in both systems, and consequently, to know more about the orbital history of the Clouds, we need a meticulous, quantitative comparison between their SFHs extending to intermediate ages, with good age precision. However, this information is still partly missing. Ruiz-Lara et al. (2020b) illustrate that the recent SFH of the LMC is not uniformly defined across the face of the stellar disc. In particular, stars in the northern edge of the disc show a marked increase in recent star formation (<0.45 Gyr) that is not mirrored in the South. This motivates an extra question on whether the localized SFH of the LMC is correlated with the global SFH of the SMC. We present here a global SFH of the SMC and compare it to the SFH obtained by Ruiz-Lara et al. (2020b) for the LMC. Both SFHs have been obtained using homogeneous data sets (SMASH survey), methodology, and reference stellar evolution models, as well as the deepest and most precise CMDs available to date, reaching well below the oldest main-sequence turnoff with excellent photometric precision and high completeness. While the homogeneous modelling procedure, and in particular, the use of the same library of stellar models, can affect the intensity or absolute age of star formation bursts in a systematic way, if the same bursts are found in both galaxies, it would indicate that they are indeed present in the data. This letter is organized as follows: In Section 2, we succinctly describe the SMASH data set used here. In Section 3 we describe the methodology used to calculate the SFHs. We present the results in Section 4, followed by the discussion in Section 5. Finally, the conclusions are presented in Section 6.

2 SMC IN SMASH

The Survey of the Magellanic Stellar History (SMASH) uses the Dark Energy Camera (DECam; Flaugher et al. 2015) on the Blanco 4-m telescope at Cerro Tololo Interamerican Observatory and was designed with the main goals of recovering the SFHs of the MCs and detecting faint stellar structures in their outskirts. Its data span the *ugriz* filters and all fields reach a depth of at least $g \sim 24$ mag (some reaching as faint as $g \sim 26$ mag). The combined depth and areal coverage are the best to date for the MCs for a single survey. We use here the second and final SMASH data release (Nidever et al. 2021), and a full description of the SMASH catalogue can be found in Nidever et al. (2017). The subset of SMASH used for this letter covers the SMC as far out as 4° from its centre, including a total of 31 deg^2 of its main body. In short, it has several columns outputted by PHOTRED, which can be used to perform the desired photometric selection. Here, we used $-2.5 < \mathrm{SHARP} < 2.5$ to reduce contamination by galaxies and spurious objects. We applied dust correction using a reddening map constructed based on the red clump method described in Choi et al. (2018), assuming an intrinsic $g - i$ colour of 0.72. We used a distance modulus for the SMC of $(m - M)_0 = 18.9$. Additionally, we performed tests using mock populations with Gaussian-like line-of-sight depths and standard deviations ranging from 0 to 5.5 kpc (similar to those observed with red clump stars by Tatton et al. 2021), showing negligible effects in the resulting SMC SFHs. This will be discussed in more detail in Sakowska et al. in preparation, and it is in good agreement with similar findings in Rubele et al. 2018 and Harris & Zaritsky 2004. The contamination by stars from the MW globular cluster 47 Tuc has been removed as in Massana et al. (2020).

3 SFH CALCULATION

We created a synthetic CMD containing 1.5×10^8 stars with uniform distributions in age ($0.03 \leq$ age [Gyr] ≤ 14) and metallicity ($0.0001 \leq Z \leq 0.025$) based on the solar-scaled BaSTI stellar evolutionary models (Pietrinferni et al. 2004). We used a Kroupa initial mass function (Kroupa 2001) and a binary fraction of 50 per cent with a mass ratio ranging from 0.1 to 1. The photometric completeness and uncertainties were derived from artificial-star tests (ASTs; e.g. Gallart, Aparicio & Vilchez 1996) following standard procedures. Artificial stars covering the range of colours, magnitudes, and sky locations sampled by the observed stars have been injected and measured in the real images. They were distributed in a regular grid on every chip, avoiding an overlap of point spread function wings. We then used the code *DisPar* (see Ruiz-Lara et al. 2021 for information) to simulate the observational effects on the synthetic CMDs.

We spatially divided the SMC SMASH data set into 74 regions with a similar number of stars (∼281 000 on average) using Voronoi binning (Cappellari & Copin 2003). They can be combined to obtain a global picture or analysed separately.

We used THESTORM (Tracing tHe Evolution of the STar fOrmation Rate and Metallicity) software (Bernard et al. 2015, 2018) to obtain the best-fitting SFH solution for each Voronoi bin. This code uses a Poisson adapted χ^2 to find the best combination of synthetic single

Downloaded from https://academic.oup.com/mnrasl/article/513/1/L40/6554248 by Biblioteca P. Arduino user on 24 June 2022

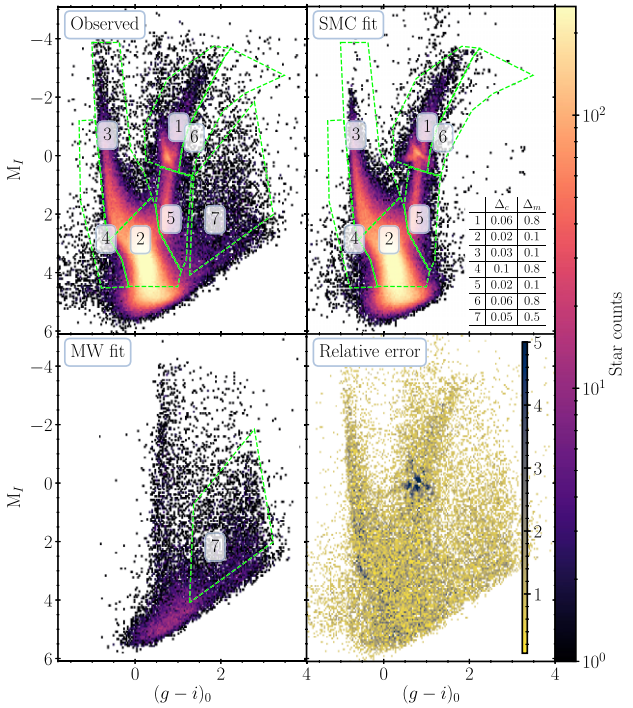

Figure 1. From left-hand to right-hand and top to bottom panels: observed CMD, best SMC CMD fit, MW fit, and relative errors (ratio between residuals and star counts). Magnitudes and colours are in the absolute plane, considering distance, reddening, and extinction. Green polygons show the 'bundle' strategy. Inset table shows the binnings applied to each bundle.

stellar populations that fit the observed distribution of stars. CMDs are divided into different areas that we call 'bundles' (see the dashed green polygons in Fig. 1), following the nomenclature introduced by Aparicio & Hidalgo (2009) and widely used since then in papers using this methodology (see Monelli et al. 2010; Bernard et al. 2012; Rusakov et al. 2021). These bundles are uniquely binned in order to give different weights in the fit depending on the amount of information we can obtain. For example, the main-sequence area where precise information on age is found is divided into smaller bins (see inset table in Fig. 1). Fig. 1 depicts a comparison between the various Hess diagrams involved in the calculation of the SFH for a typical SMC Voronoi bin (1.75° from the centre). Uncertainties in the SFR are determined as described in detail in Rusakov et al. (2021), which in turn follows the prescriptions in Hidalgo et al. (2011). The metallicity fit, although not represented in this manuscript, has been compared to literature results obtained using MC clusters and good agreement is found.

MW foreground contamination was modelled using THESTORM by inputting a field located far from the SMC main body (number 139 in Nidever et al. 2021) and scaling it through the same fitting procedure, using a bundle only populated by MW halo stars (bundle 7 in Fig. 1).

4 RESULTS

4.1 SMC global SFH

To obtain a global SFH for the SMC, we combined the SFHs from all Voronoi bins that reach 50 per cent completeness at a magnitude of $M_I = 2.5$ or fainter. We excluded the shallowest fields (6 bins out of 74) to avoid the severe crowding in the SMC centre. To assess our capability to discern independent periods of enhanced star formation (that is, to estimate our age resolution), we created several mock populations containing only stars in instantaneous peaks at particular ages. We simulated observational uncertainties with *DisPar* and then applied THESTORM to compute recovered age distributions. The top panel of Fig. 2 shows the global SFH for the SMC; the horizontal bars represent the recovered width (full width at half-maximum of the instantaneous peaks in star formation rate (SFR) at each look-back time.

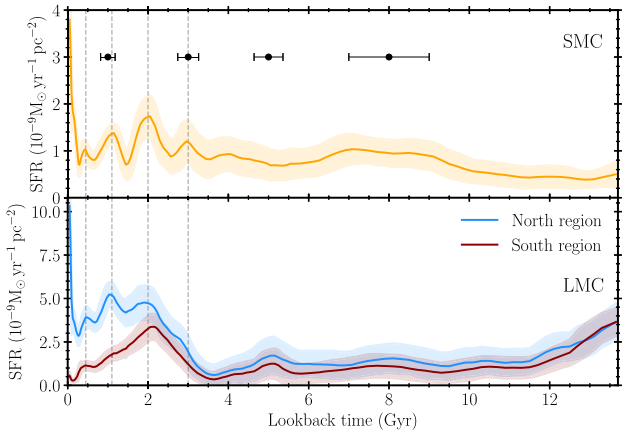

Figure 2. Comparison of the global SFRs for the SMC (this work) and the LMC (Ruiz-Lara et al. 2020b). Vertical dashed lines link the peaks at 0.45, 1.1, 2, and 3 Gyr ago in the SMC to those of the LMC. The horizontal bars in the top panel show the width of the SFH enhancement. Uncertainties in the SFHs (shaded regions) were calculated as in Hidalgo et al. (2011) and Rusakov et al. (2021).

The recovered, global SFH shows five main conspicuous peaks, at ∼3, ∼2, ∼1.1, and ∼0.45 Gyr ago, as well as an ongoing one. There is also a minor but extended (in time) increment in the SFR between ∼6.5 and ∼9 Gyr ago. There is no evidence of a period of early (i.e. earlier than 10 Gyr ago) enhanced star formation in the SMC, in contrast to the case of the LMC (Monteagudo et al. 2018).

4.2 Comparison of the SFHs and spatial stellar distribution between the MCs

In order to investigate the potential effects that interactions have on the SFHs of the LMC and SMC, we compared the global SFH obtained here with those obtained in Ruiz-Lara et al. (2020b), also using SMASH survey data and the same methodology. In the bottom panel of Fig. 2, LMC SFHs are displayed for both the North (blue line) and the South (red line) regions of the LMC. The peaks in the SFHs of the SMC and those of the LMC North region show a clear synchronization, indicating a common evolution of the pair since at least ∼3.5 Gyr ago. The pronounced peak found in the SMC at ∼2 Gyr ago coincides with peaks found in the LMC's SFR in both the North and the South regions. This is likely linked to an interaction between the MCs around 2 Gyr ago that might have triggered intense star formation over the whole main body of both galaxies. The period of enhanced star formation at intermediate/old ages (6–10 Gyr) in the SMC does not have a clear counterpart in the LMC. Given the calculated widening of an SFR peak at around 8 Gyr ago, represented by the error bars on the top part of the figure, it is possible that the SFH 7–9 Gyr ago was much more structured than shown in Fig. 2. Indeed, Tsujimoto & Bekki (2009) suggest a major merger event occurred at the SMC 7.5 Gyr ago. By comparison, the apparent lack

Downloaded from https://academic.oup.com/mnrasl/article/513/1/L40/6554248 by Biblioteca P. Arduino user on 24 June 2022

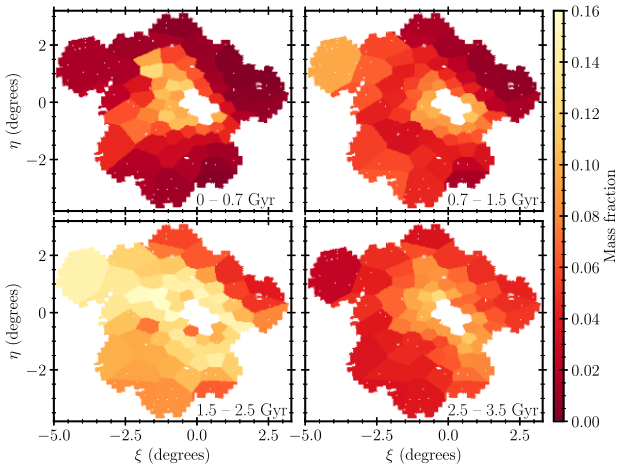

Figure 3. Sky distribution of the stellar mass fraction formed in the SMC. The mass fraction is calculated from the SFH of each bin. Age bins were chosen to match the periods of enhanced SFR seen in Fig. 2. The central bins are in white because they have been left out due to intense crowding.

of enhanced star formation in the LMC in this period would suggest that interactions between the MCs commenced no earlier than 6–7 Gyr ago.

To better understand how the interaction with the LMC might have triggered star formation episodes in the SMC, we followed the analysis introduced by Ruiz-Lara et al. (2020b). First, we calculated the mass fraction of stars formed in each of the episodes with respect to the total SMC SFH and plotted it as a function of Voronoi bin as shown in Fig. 3. The Eastern SMC bins (towards the LMC), are the predominant locations for star formation in the last 0.7 Gyr, probably corresponding to the last LMC-SMC interaction ∼0.2 Gyr ago. The stars produced in the burst 2 Gyr ago are distributed almost everywhere in the SMC, in contrast with the predominantly centrally concentrated star formation in the other periods. We highlight how specific interactions between the MCs have different effects on the LMC and SMC. The most prominent burst of star formation in both galaxies is that at ∼2 Gyr when the star formation appears to be more global in both systems. We note though, that these stars have mixed after 2 Gyr of evolution, contributing to a wider distribution. At the more recent ages (<2 Gyr), the star formation continues to be more global and centrally concentrated in the SMC (mimicking the mass distribution of the least massive system of the two), whereas the star formation in the LMC is localized towards the northern part (see Fig. 3 in Ruiz-Lara et al. 2020b).

5 DISCUSSION

5.1 Comparison with the literature

Previous studies of SFHs of the MCs have covered a variety of areas and depths, from studies centred on several very small areas of the MCs with very deep photometry (e.g. Noël et al. 2009, Cignoni et al. 2012, Weisz et al. 2013, Meschin et al. 2014), to very wide field studies with shallower photometric depths (e.g. Harris & Zaritsky 2004, Harris & Zaritsky 2009, Rubele et al. 2018, Mazzi et al. 2021). Our results offer the best compromise, to date, between a large coverage of the MCs and a photometric depth that is able to reach the oldest MSTO of both galaxies with unprecedented depth. This fact allows for a much improved age resolution in the global SFH with respect to results present in the literature. To put our synchronous

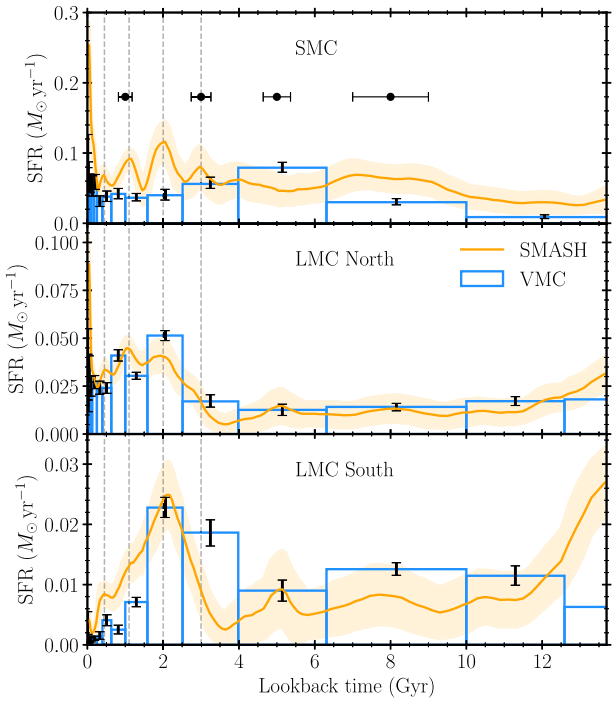

Figure 4. Comparison of the SFHs obtained by the SMASH and VMC (Cioni et al. 2011) surveys. For the SMC, we compare our results with those of Rubele et al. (2018). For the LMC, we have used two subsets of the results obtained by Mazzi et al. (2021) to compare with the results from Ruiz-Lara et al. (2020b). See Fig. 2 for details.

SFH determinations in the context of the current knowledge, we compare them with global studies of the MCs from Harris & Zaritsky (2004, 2009; hereafter HZ04 and HZ09, respectively) and from the VMC survey (Cioni et al. 2011): Rubele et al. (2018, hereafter R18) for the SMC and Mazzi et al. (2021, hereafter M21) for the LMC.

A direct comparison of our SMC SFH and that of Ruiz-Lara et al. (2020b) for the LMC, with those obtained by the VMC team, is displayed in Fig. 4. Given that SMASH covers a larger area than VMC in the SMC, we added all VMC fields in the SFH represented in 4 (no scaling applied), resulting in a somewhat lower SFR for VMC. For the LMC, we selected SFHs from VMC tiles overlapping the area where the LMC north and south regions were defined by Ruiz-Lara et al. (2020b), i.e. tiles 8_7, 8_6, 8_5, 8_4, 8_3, 7_2, 7_3, 6_2 and 5_8, 4_8, 4_7, 3_7, 3_6, 3_5, 3_4, 4_4, respectively. We used their SFH solutions from JK_s photometry.

A comparison between the SFHs obtained by HZ and VMC has been performed in R18 for the SMC and in M21 for the LMC. While there is a fair agreement between these two previous works in the case of the LMC (see fig. 16 in M21), with both studies found an increase in the SFH around 3 Gyr ago (also in agreement with Ruiz-Lara et al. 2020b; see Fig. 4), the correspondence between the features in the SMC SFH by HZ04 and R18 is quite poor (see fig. 11 in R18). For example, HZ04 also find an increase in the SFR around 3 Gyr ago, while this is not found in the R18 solutions. This discrepancy also exists in the comparison between the SMC SFH presented in this paper and that of R18 (see below).

Owing to our improved age resolution at intermediate ages, the solutions presented in this work and in Ruiz-Lara et al. (2020b) display a variety of details in the form of the star formation peaks that are not captured by the previous results. Fig. 4 shows a reasonable

Downloaded from https://academic.oup.com/mnrasl/article/513/1/L40/6554248 by Biblioteca P. Arduino user on 24 June 2022

agreement for the LMC, with both surveys being able to recover the main peak of star formation ∼2 Gyr ago and some hints of the peaks at ∼1 and 0.45 Gyr ago. The onset of the epoch of increased SFR around 3.5 Gyr ago is more precisely dated with the SMASH SFHs. The episodic SFH presented here for the SMC contrasts with the smoothness of that from R18. Note that due to the larger distance of the SMC (∼0.4 mag further away than the LMC), its 10 Gyr old main-sequence turnoff lies very close to the 50 per cent SMC VMC completeness limit at ∼ K_s =21. The peaks at ∼5 Gyr and ∼7–9 Gyr were not seen in previous surveys.

Here, we improve the constraints of the enhancements at ∼0.5 and 2 Gyr ago found by HZ and add a peak at ∼ 1 Gyr not found in their work. Additionally, we can more precisely date the re-ignition of star formation in both MCs as occurring 3.5 Gyr ago, rather than 5 Gyr ago as established in HZ09, which we believe is due to their coarser age resolution at intermediate and old ages. Note that there is a plausible peak in the SFR of the LMC ∼5 Gyr ago, not seen in the SMC. This could indicate that the MCs were not interacting at those times, which would also explain not seeing the ∼7–9 Gyr in the LMC that is evident in the SMC.

5.2 Implications for the LMC-SMC system

Simulations of dynamical interactions provide much of our insight into the history of the MCs; however, such simulations necessarily must account for observational constraints such as the characteristics of the Magellanic Stream and Bridge. Proper motions and radial velocities (combined with distances) are able to aid in the selection of initial conditions as well as to obtain possible masses and orbits for the MCs (e.g. Zivick et al. 2018; Patel et al. 2020). Under the assumption that galaxy interactions drive star formation, the synchronicity of the MCs SFHs reported in this work adds a new layer of observational constraints to improve our knowledge of their orbital configuration. Indeed, in recent years a number of works have discussed the effects (mainly enhancements) of interactions on SFHs (see e.g. Ruiz-Lara et al. 2020a, 2021; Di Cintio et al. 2021; Rusakov et al. 2021)

The SMC SFH presented here, combined with the SFH of the LMC from Ruiz-Lara et al. (2020b), suggests a common evolution of both galaxies for, at least, the past ∼3.5 Gyr. The fact that the precise timing of star formation enhancements is simultaneous in both MCs can be interpreted as the times when they experienced close encounters at ∼0.45, 1, 2, and 3 Gyr ago. Note that the star formation enhancements are found to be 1 Gyr apart except for the last Gyr when interactions are separated by only ∼0.5 Gyr. This agrees with the expectations from numerical models that predict the time-scale of repeated encounters to decrease towards recent times due to dynamical friction (e.g. see Murai & Fujimoto 1980, Bekki & Chiba 2005, Růžička, Theis & Palouš 2010, Besla et al. 2012). Besides, in the past 0.5 Gyr, the effect of the MW on the MCs orbits is thought to have increased (see Besla et al. 2007; Patel et al. 2020). Our findings also indicate that in spite of their mass difference (e.g. Cox et al. 2008), the SMC has been able to induce star formation on the LMC, although mainly locally (the northern edge of the LMC closest to the SMC) rather than globally. The exception to this is the encounter 2 Gyr ago that coincides with the epoch when the SMC was tidally truncated (Massana et al. 2020) and with the formation of the LMC bar (Ruiz-Lara et al. 2020b). Finally, we highlight that these results seem to suggest the northern LMC disc as the most probable SMC-LMC impact site for the most recent interaction (direct impact evidence :Bekki 2009; Besla et al. 2012; Noël et al. 2013; Zivick et al. 2018).

6 CONCLUSIONS

We present here the spatially resolved SFH for the SMC computed from SMASH data, with greatly improved age resolution from previous studies. This SMC SFH was compared to that obtained for the LMC previously by Ruiz-Lara et al. (2020b), finding that both MCs show correlated SFR episodes, with enhancements in their SFHs at ∼3, ∼2, ∼1.1, ∼0.45 Gyr ago and currently. We were able to discern individual bursts of star formation in unprecedented detail, allowing us to unequivocally demonstrate that the SMC and LMC have been interacting and mutually influencing each other for at least the past ∼3.5 Gyr. We found that the separation between enhancements indicates a possible orbital period of around 1 Gyr, in agreement with dynamical studies (Kallivayalil et al. 2013), though dynamical friction may have shortened such period to 0.5 Gyr for the last two passages. Owing to their mass difference, the SFR enhancements in the SMC are global while in the LMC are mainly concentrated in the northern part, with the exception of the burst 2 Gyr ago.

To conclude, using the power of our full-body determination of the SFHs of both MCs, we established constraints on their interaction history, finding that the SMC and the LMC had a synchronized dance that has been taking place for the last ∼3.5 Gyr. These constraints on the MCs' orbits have implications on the masses of the MW and the MCs themselves and are potential probes of the influence of interactions on the onset and strength of induced star formation.

ACKNOWLEDGEMENTS

PM thanks for the hospitality of the IAC during the Erasmus + placement. This research uses services or data provided by the Astro Data Lab at NSF's National Optical-Infrared Astronomy Research Laboratory. NSF's OIR Lab is operated by the Association of Universities for Research in Astronomy (AURA), Inc. under a cooperative agreement with the National Science Foundation. TRL acknowledges support from a Spinoza grant (NWO) awarded to A. Helmi. CG and MM acknowledge financial support through the grants (AEI/FEDER, UE) AYA2017-89076-P and PID2020-118778GB-I00. GB acknowledges support from the NSF under grant AST 1714979. SC acknowledges support from Premiale INAF MITiC, from INFN (Iniziativa specifica TAsP), and from PLATO ASI-INAF agreement n.2015-019-R.1-2018. MRC acknowledges support from the European Research Council (ERC) under the European Union Horizon 2020 research and innovation programme (grant agreement no. 682115). AM acknowledges support from FONDECYT Regular grant 1212046 and funding from the Max Planck Society through a 'PartnerGroup' grant.

DATA AVAILABILITY

The photometry of SMASH used in this study can be accessed at https://datalab.noirlab.edu/smash/smash.php. This research uses services or data provided by the Astro Data Lab at NSF's NOIRLab. NOIRLab is operated by the Association of Universities for Research in Astronomy (AURA), Inc. under a cooperative agreement with the National Science Foundation. All data products can be provided upon reasonable request to the corresponding author.

REFERENCES

Aparicio A., Hidalgo S. L., 2009, AJ, 138, 558
Bekki K., 2009, MNRAS, 393, L60

Downloaded from https://academic.oup.com/mnrasl/article/513/1/L40/6554248 by Biblioteca P. Arduino user on 24 June 2022

Bekki K., Chiba M., 2005, MNRAS, 356, 680
Bekki K., Chiba M., 2007, PASA, 24, 21
Bernard E. J. et al., 2012, MNRAS, 420, 2625
Bernard E. J., Ferguson A. M. N., Chapman S. C., Ibata R. A., Irwin M. J., Lewis G. F., McConnachie A. W., 2015, MNRAS, 453, L113
Bernard E. J., Schultheis M., Di Matteo P., Hill V., Haywood M., Calamida A., 2018, MNRAS, 477, 3507
Besla G., Kallivayalil N., Hernquist L., Robertson B., Cox T. J., van der Marel R. P., Alcock C., 2007, ApJ, 668, 949
Besla G., Kallivayalil N., Hernquist L., van der Marel R. P., Cox T. J., Kereš D., 2012, MNRAS, 421, 2109
Brüns C. et al., 2005, A&A, 432, 45
Cappellari M., Copin Y., 2003, MNRAS, 342, 345
Carrera R., Conn B. C., Noël N. E. D., Read J. I., López Sánchez Á. R., 2017, MNRAS, 471, 4571
Choi Y. et al., 2018, ApJ, 866, 90
Cignoni M., Cole A. A., Tosi M., Gallagher J. S., Sabbi E., Anderson J., Grebel E. K., Nota A., 2012, ApJ, 754, 130
Cioni M. R. L. et al., 2011, A&A, 527, A116
Cox T. J., Jonsson P., Somerville R. S., Primack J. R., Dekel A., 2008, MNRAS, 384, 386
Cullinane L. R. et al., 2020, MNRAS, 497, 3055
De Leo M., Carrera R., Noël N. E. D., Read J. I., Erkal D., Gallart C., 2020, MNRAS, 495, 98
Di Cintio A., Mostoghiu R., Knebe A., Navarro J., 2021, MNRAS, 506, 531
Ellison S. L., Mendel J. T., Patton D. R., Scudder J. M., 2013, MNRAS, 435, 3627
Flaugher B. et al., 2015, AJ, 150, 150
Gaia Collaboration et al., 2021, A&A, 649, A7
Gallart C., Aparicio A., Vilchez J. M., 1996, AJ, 112, 1928
Glatt K. et al., 2008, AJ, 135, 1106
Graczyk D. et al., 2020, ApJ, 904, 13
Harris J., Zaritsky D., 2004, AJ, 127, 1531 (HZ04)
Harris J., Zaritsky D., 2009, AJ, 138, 1243 (HZ09)
Hidalgo S. L. et al., 2011, ApJ, 730, 14
Hindman J. V., Kerr F. J., McGee R. X., 1963, Aust. J. Phys., 16, 570
Kallivayalil N., van der Marel R. P., Alcock C., Axelrod T., Cook K. H., Drake A. J., Geha M., 2006a, ApJ, 638, 772
Kallivayalil N., van der Marel R. P., Alcock C., 2006b, ApJ, 652, 1213
Kallivayalil N., van der Marel R. P., Besla G., Anderson J., Alcock C., 2013, ApJ, 764, 161
Kroupa P., 2001, MNRAS, 322, 231
Mackey A. D., Koposov S. E., Erkal D., Belokurov V., Da Costa G. S., Gómez F. A., 2016, MNRAS, 459, 239
Massana P. et al., 2020, MNRAS, 498, 1034
Mastropietro C., Moore B., Mayer L., Wadsley J., Stadel J., 2005, MNRAS, 363, 509
Mazzi A. et al., 2021, MNRAS, 508, 245 (M21)
Meschin I., Gallart C., Aparicio A., Hidalgo S. L., Monelli M., Stetson P. B., Carrera R., 2014, MNRAS, 438, 1067
Monelli M. et al., 2010, ApJ, 720, 1225
Monteagudo L., Gallart C., Monelli M., Bernard E. J., Stetson P. B., 2018, MNRAS, 473, L16
Murai T., Fujimoto M., 1980, PASJ, 32, 581
Nidever D. L., Majewski S. R., Butler Burton W., Nigra L., 2010, ApJ, 723, 1618
Nidever D. L. et al., 2017, AJ, 154, 199
Nidever D. L. et al., 2021, AJ, 161, 74
Noël N. E. D., Gallart C., Costa E., Méndez R. A., 2007, AJ, 133, 2037
Noël N. E. D., Aparicio A., Gallart C., Hidalgo S. L., Costa E., Méndez R. A., 2009, ApJ, 705, 1260
Noël N. E. D., Conn B. C., Carrera R., Read J. I., Rix H. W., Dolphin A., 2013, ApJ, 768, 109
Noël N. E. D., Conn B. C., Read J. I., Carrera R., Dolphin A., Rix H. W., 2015, MNRAS, 452, 4222
Olszewski E. W., Schommer R. A., Suntzeff N. B., Harris H. C., 1991, AJ, 101, 515
Patel E. et al., 2020, ApJ, 893, 121
Pietrinferni A., Cassisi S., Salaris M., Castelli F., 2004, ApJ, 612, 168
Pietrzyński G. et al., 2019, Nature, 567, 200
Rubele S. et al., 2018, MNRAS, 478, 5017 (R18)
Ruiz-Lara T., Gallart C., Bernard E. J., Cassisi S., 2020a, Nat. Astron., 4, 965
Ruiz-Lara T. et al., 2020b, A&A, 639, L3
Ruiz-Lara T. et al., 2021, MNRAS, 501, 3962
Rusakov V., Monelli M., Gallart C., Fritz T. K., Ruiz-Lara T., Bernard E. J., Cassisi S., 2021, MNRAS, 502, 642
Růžička A., Theis C., Palouš J., 2010, ApJ, 725, 369
Schmidt T. et al., 2020, A&A, 641, A134
Tatton B. L. et al., 2021, MNRAS, 504, 2983
Tsujimoto T., Bekki K., 2009, ApJ, 700, L69
Weisz D. R., Dolphin A. E., Skillman E. D., Holtzman J., Dalcanton J. J., Cole A. A., Neary K., 2013, MNRAS, 431, 364
Zivick P. et al., 2018, ApJ, 864, 55

This paper has been typeset from a TEX/LATEX file prepared by the author.

Downloaded from https://academic.oup.com/mnrasl/article/513/1/L40/6554248 by Biblioteca P. Arduino user on 24 June 2022